Dynamic and reversible restructuring of the ER induced by PDMP in cultured cells

Teresa Sprocati[1], Paolo Ronchi[1], Andrea Raimondi[1,*], Maura Francolini[1] and Nica Borgese[1,2,‡]

[1]Consiglio Nazionale delle Ricerche Institute of Neuroscience and Department of Medical Pharmacology, via Vanvitelli 32, University of Milano, 20129 Milano, Italy
[2]Department of Pharmacobiological Science, 'Magna Graecia' University of Catanzaro, 88100 Catanzaro, Italy
*Present address: Department of Cell Biology, Howard Hughes Institute for Medical Research, Yale University School of Medicine, PO Box 208002, New Haven, CT 06520, USA
‡Author for correspondence (e-mail: n.borgese@in.cnr.it)

Accepted 18 May 2006
Journal of Cell Science 119, 3249-3260 Published by The Company of Biologists 2006
doi:10.1242/jcs.03058

Summary

In many cells, the endoplasmic reticulum (ER) contains segregated smooth and rough domains, but the mechanism of this segregation is unclear. Here, we used a HeLa cell line, inducibly expressing a GFP fusion protein [GFP-b(5)tail] anchored to the ER membrane, as a tool to investigate factors influencing ER organisation. Induction of GFP-b(5)tail expression caused proliferation of the ER, but its normal branching polygonal meshwork architecture was maintained. Experiments designed to test the effects of drugs that alter ceramide levels revealed that treatment of these cells with Phenyl-2-decanoyl-amino-3-morpholino-1-propanol-hydrocholride (PDMP) generated patches of segregated smooth ER, organised as a random tubular network, which rapidly dispersed after removal of the drug. The effect of PDMP was independent of its activity as sphingolipid synthesis inhibitor, but could be partially reversed by a membrane-permeant Ca^{2+} chelator. Although the smooth ER patches maintained connectivity with the remaining ER, they appeared to represent distinct domains differing in protein and lipid composition from the remaining ER. PDMP did not cause detachment of membrane-bound ribosomes, indicating that smooth ER patch generation was due to a reorganisation of pre-existing ribosome-free areas. Our results demonstrate a dynamic relationship between smooth and rough ER and have implications for the mechanisms regulating ER architecture.

Supplementary material available online at
http://jcs.biologists.org/cgi/content/full/119/15/3249/DC1

Key words: HeLa TetOff cells, Membrane proliferation, Rough ER, Smooth ER, Tail-anchored GFP

Introduction

The endoplasmic reticulum (ER) is a single but pleiomorphic organelle containing architecturally and functionally distinct subdomains. The most clearly recognisable and well-known subcompartments are the nuclear envelope and the peripheral ER; within the latter, rough (ribosome-covered) and smooth (ribosome-free) regions (RER and SER) constitute additional subdomains (Kepes et al., 2005; Voeltz et al., 2002; illustrated in Fawcett, 1981). In many cells, however, RER and SER do not occupy spatially segregated regions, and small ribosome-free areas are interspersed with ribosome-covered regions. This type of ER is generally organised in sheets (cisternae) or in a branching tubular network typically seen in many cultured mammalian cells. Such networks are characterised by fairly straight tubules, which branch at tripartite junctions to generate a polygonal meshwork (Kepes et al., 2005; Terasaki et al., 1984). Only in some cells (e.g. hepatocytes or steroid-synthesising cells), do smooth and rough portions of the ER occupy different regions of the cytoplasm. In these cases, the SER is distinguished from the RER on the basis not only of its ribosome-free surface but also of its particular architecture.

Different architectural forms of SER are observed in different cells and under varying conditions. In cultured cells overexpressing ER membrane proteins that have the capacity for head-to-head dimerisation of their cytosolic domains, SER forms parallel arrays of stacked cisternae – organised smooth ER (OSER) (Snapp et al., 2003) – which may be lined up against the nuclear envelope (karmellae), form whorls, or be organised as cubic or hexagonal 'crystalloid' ER (Anderson et al., 1983). Such stacked SER cisternae are also seen in some tissues (e.g. cerebellar Purkinje cells) (Takei et al., 1994). More commonly, however, SER forms a tubular network with characteristics that are quite different from those of the polygonal meshwork described above for RER. The SER tubules are generally more convoluted than those of RER, and the branch points are more frequent, so that a sponge-like structure is generated (Kepes et al., 2005; Fawcett, 1981). We refer to this SER architecture as 'random tubular'. Notwithstanding the decades that have passed since the distinction between smooth and rough ER was first made (Palade, 1956), the molecular basis of ER differentiation into the random tubular or polygonal meshwork/sheet organisation has remained enigmatic.

One way to investigate the genesis of ER architecture is to treat cells with drugs that alter the organisation of the organelle. For instance, calcium ionophores and nocodazole (an inhibitor of microtubule polymerisation) both disrupt ER organisation (Subramanian and Meyer, 1997; Terasaki et al., 1986), implying that the cytosolic Ca^{2+} concentration and ER

interaction with the cytoskeleton are important for the spatial distribution and maintenance of the network.

Because the formation of membranous tubules, a hallmark of ER architecture, may depend on lipid composition (for reviews, see Farsad and De Camilli, 2003; McMahon and Gallop, 2005), the effects of drugs that target lipid metabolism are also of potential interest for the investigation of ER architecture. The ER is the major site of synthesis of membrane lipids of the cell, so that its own lipid composition is dependent on a fine balance between synthesis, export and degradation. For instance, in animal cells ceramide, the precursor of sphingomyelin and of glycolipids, is synthesised in the ER, where its concentration is kept low because of its export to the Golgi complex. In the Golgi complex it is used by the enzymes glucosylceramide synthase and sphingomyelin synthase to generate more complex sphingolipids (reviewed by Futerman and Riezman, 2005). 1-Phenyl-2-decanoyl-amino-3-morpholino-1-propanol hydrochloride (PDMP) is a drug that inhibits both these enzymes (Rosenwald et al., 1992; Vunnam and Radin, 1980), with a consequent elevation of intracellular ceramide concentrations. PDMP interferes with transport from the ER to the Golgi (Maceyka and Machamer, 1997; Rosenwald et al., 1992) as well as with Brefeldin-A-induced retrograde transport from the Golgi to the ER (Kok et al., 1998). The effect of the drug on ER-to-Golgi transport is thought to be a direct consequence of the inhibition of ceramide consumption (Maceyka and Machamer, 1997; Rosenwald et al., 1992). Other effects of PDMP, however, appear to be independent from its action as sphingolipid synthesis inhibitor (De Matteis et al., 1999; Griner and Bollag, 2000; Kok et al., 1998).

In the present study, we carried out experiments aimed at testing the effect on ER architecture of drugs that alter intracellular ceramide levels, and found that PDMP produces a dramatic reorganisation of the organelle in a HeLa cell line expressing a GFP fusion protein anchored to the ER membrane. Although the underlying mechanism of this phenomenon turned out to be independent of PDMP activity as a sphingolipid biosynthesis inhibitor, we exploited this novel effect of the drug to investigate dynamic changes in ER organisation. We found that in these cells PDMP induces the segregation of patches of SER, organised as a random tubular network, which are continuous with the polygonal meshwork, partially exclude rough ER proteins, and are rapidly dispersed upon removal of the drug. The results illustrate the capacity of ER to rapidly reorganise its architecture in response to altered conditions, and provide a model system which may prove useful to investigate the molecular basis of the segregation between rough and smooth domains of the ER.

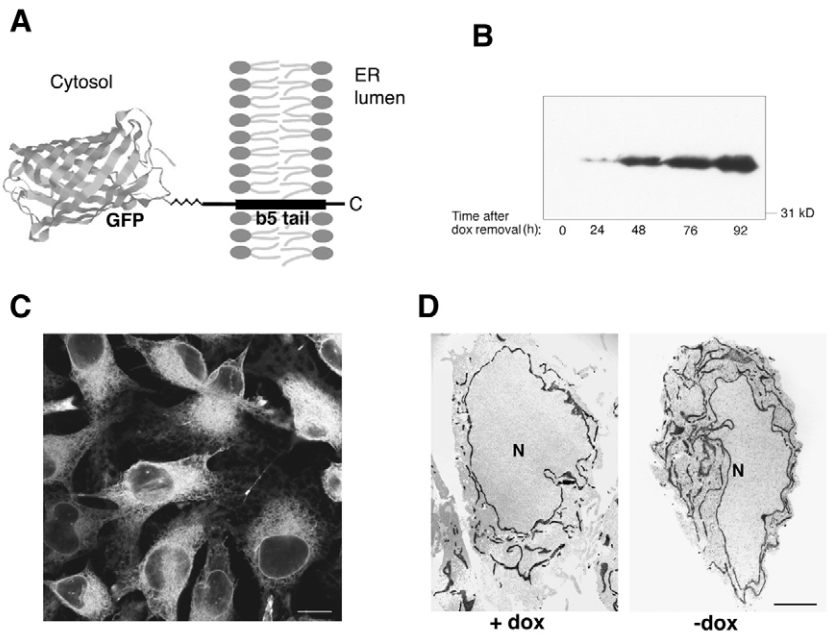

Fig. 1. Illustration of GFP-b(5)tail and characterisation of HeLa TetOff cells expressing the construct. (A) Schematic representation of GFP-b(5)tail. The construct is composed of GFP fused at its C-terminus to a linker (zig-zagged line) consisting of the *myc* epitope followed by a repeated Gly-Ser sequence. This is attached to the entire tail region of rat cytochrome b(5), which contains the transmembrane domain flanked upstream and downstream by polar sequences. The orientation of the construct, with the N-terminal GFP in the cytosol and the C-terminus in the ER lumen is indicated. (B) Western blot analysis of GFP-b(5)tail expression in stably transfected HeLa TetOff cells. Cells were harvested at the indicated times after removal of doxycycline from the culture medium. Each lane contained 55 μg of protein. (C) Confocal analysis of HeLa TetOff cells expressing GFP-b(5)tail. Cells were fixed 3 days after exposure to doxycycline-free medium. Bar, 10 μm. (D) G-6-Pase EM cytochemistry of HeLa TetOff cells, induced (right) or not induced (left) to express GFP-b(5)tail. The product of the cytochemical reaction is found within the nuclear envelope and in ER cisternae. Note the higher density of ER cisternae in the induced cells. N, nucleus. Bar, 1 μm.

Results

Characterisation of HeLa TetOff cells with inducible expression of an ER tail-anchored protein

To generate a tool that would allow easy visualisation of changes in ER organisation, we produced a cell line stably expressing an ER-targeted GFP fusion protein. We chose a well-characterised construct, GFP-b(5)tail, which we have used in previous work to investigate transmembrane domain-dependent intracellular sorting (Bulbarelli et al., 2002) and ER plasticity (Snapp et al., 2003). As illustrated in Fig. 1A, GFP-b(5)tail consists of a cytosolically located EGFP fused at its C-terminus to the membrane anchor of cytochrome b(5). Because cell lines with constitutive expression of this protein lost the capacity to produce it with time in culture, we generated a TetOff cell line with inducible expression (Gossen and Bujard, 1992). These cells were kept in culture with GFP-b(5)tail expression repressed by doxycycline, and maintained the capacity to express the construct upon removal of the antibiotic (Fig. 1B).

We first examined the ER of induced cells by confocal microscopy. Three days after removal of doxycycline from the culture medium, GFP fluorescence revealed a normal ER staining pattern (Fig. 1C), which persisted for up to 2 weeks of culture in the absence of the antibiotic (not shown). The normal

Table 1. Induction of GFP-b(5)tail expression causes an increase in ER surface area in HeLa TetOff cells

Treatment	ER surface area†
+ doxycycline	2.07±0.14** (*n*=13)
– doxycycline	3.59±0.27 (*n*=14)
– doxycycline + PDMP	4.44±0.48 (*n*=10)

†Surface area was estimated on electron micrographs of cells treated for cytochemical detection of G-6-Pase (see Figs 1 and 4) and normalized to total cytoplasmic volume as described by Griffiths (Griffiths, 1993). Shown are mean values ± s.e.m. Comparison of the surface areas of three groups of cells was carried out by one-way ANOVA and Tukey's multiple comparison test. **P<0.01, highly significant difference between non-expressing cells and GFP-b(5) tail-expressing cells (treated or not with PDMP).

appearance of the ER was unexpected, because our previous transient transfection experiments had shown that, at concentrations above a critical threshold value, GFP-b(5)tail induces the formation of stacked smooth cisternae (OSER) through head-to-head dimerisation of its cytosolic domain (Snapp et al., 2003). The absence of such an effect in the HeLa TetOff cell line can be explained by the lower expression levels attained in stably transfected cells compared with transiently transfected cells.

Although the ER pattern in the induced cells appeared normal by confocal microscopy, qualitative observations suggested that the density of the network increased with time of induction. To confirm that GFP-b(5)tail expression induces ER proliferation, we analysed ER surface extension by glucose-6-phosphatase (G-6-Pase) electron microscopy (EM) cytochemistry in induced and non-induced cells. As shown in Fig. 1D, the density of G-6-Pase-positive ER tubules or cisternae was indeed increased in the induced cells. Quantitative estimation carried out on images like those in Fig. 1D revealed that the ER surface area normalised to cytoplasmic volume in the induced cells was nearly twice as high as in the non-induced ones (Table 1).

PDMP induces the formation of SER patches that are continuous with the rest of the ER

To investigate whether interference with sphingolipid synthesis would alter GFP-b(5)tail localisation or ER structure, we treated the induced HeLa cells with three different inhibitors of sphingolipid synthesis: β-chloroalanine, fumonensin B1, and PDMP. Whereas the first two had no observable effect, 2-3 hours of treatment with 50-100 μM PDMP caused the appearance in 60-70% of cells of large GFP-positive structures (up to 5 μm in diameter), which coexisted with the normal polygonal meshwork (Fig. 2A and supplementary material Movie 1). The structures represented ER subdomains, as demonstrated by the presence of calnexin, an ER membrane protein, within them (Fig. 2B). At high magnification, ER tubules could be seen to emerge (or run into) the patches, suggesting their continuity with the surrounding ER (Fig. 2D). The patches extended from the basal to the apical surface of the cells so that their height tapered from internal cell regions towards the periphery, as shown in the vertical section of Fig. 2E. The appearance of other organelles was not grossly affected by PDMP, as illustrated for the Golgi complex in Fig. 2C (see also supplementary material Fig. S2).

We confirmed the continuity of the patches with the

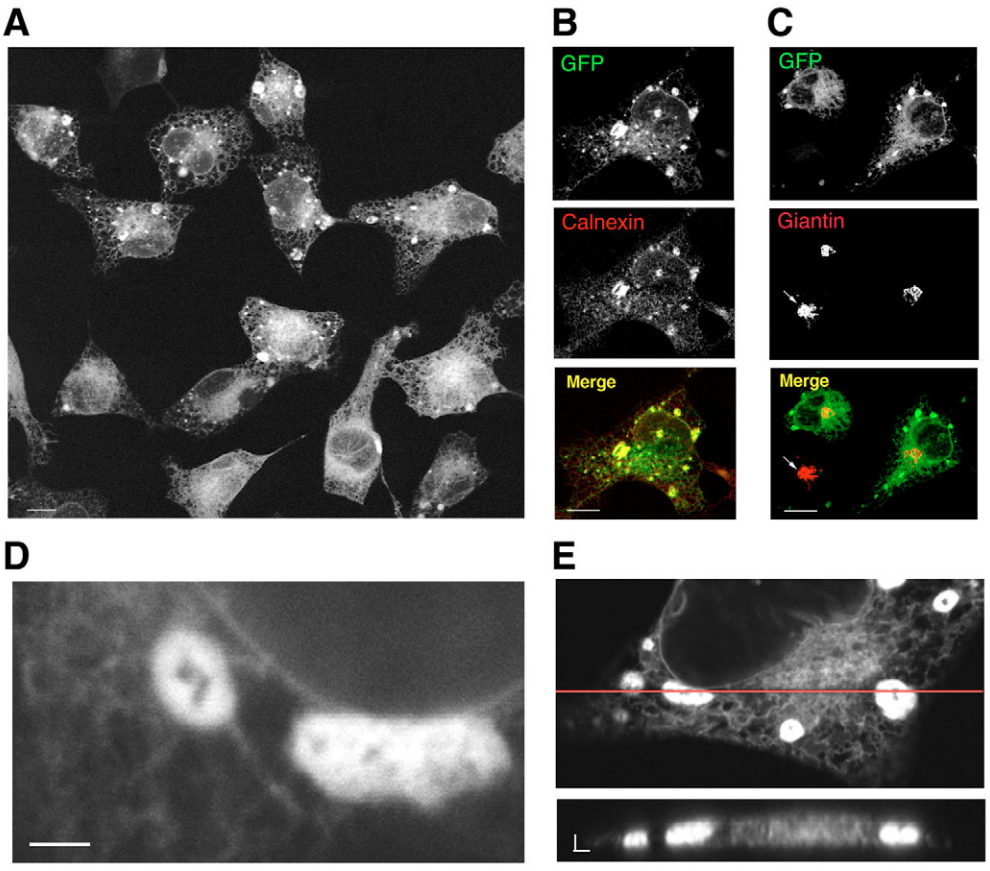

Fig. 2. Effect of PDMP on the ER of HeLa cells expressing GFP-b(5)tail. Cells grown without doxycycline for 3 days were treated with 100 μM PDMP for 3 hours, then fixed and examined by confocal microscopy, either without further manipulation (A,D,E), or after immunostaining for calnexin (B) or giantin (C), with the use of Texas-Red-conjugated secondary antibodies. Note the presence of calnexin in the PDMP-induced structures (B), and the normal appearance of the Golgi complex (C), which is similar in GFP-expressing and non-expressing cells (the latter indicated by an arrow in the middle and lower images of C). (D) PDMP-induced ER patches at higher magnification. (E) Vertical section of a cell with PDMP-induced ER patches (lower panel) and a horizontal section of the same cell (upper panel). The red line indicates the y position along which the x-z scan was performed. Bars, 10 μm (A-C); 2 μm (D-E).

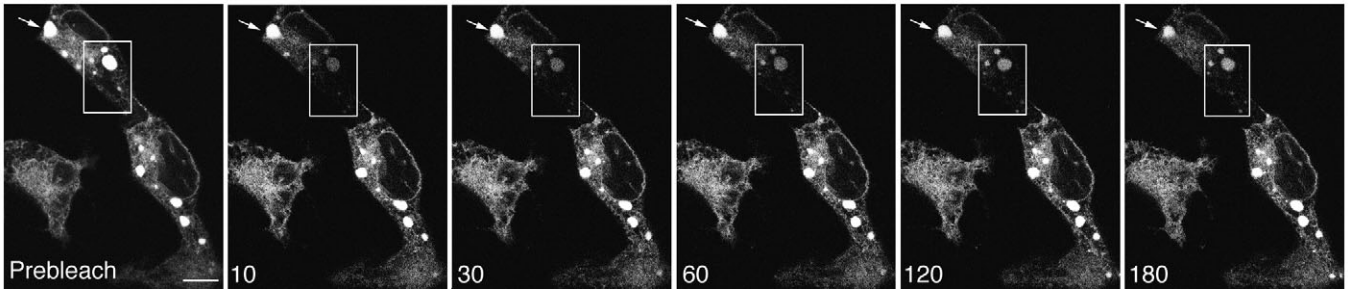

Fig. 3. FRAP analysis of PDMP-induced SER patches. The area delimited by the rectangle was bleached with unattenuated laser power and the cells were then imaged at low laser power for 3 minutes following the bleach. The numbers in the lower left corner of the panels indicate the time (in seconds) after returning to low laser power. Note that three SER patches within the boxed area recovered fluorescence at the expense of another SER patch indicated by the arrow. This effect was not due to bleaching, because the fluorescence of two other cells in the field remained constant during the imaging. Bar, 10 μm. The movie of this experiment is shown in supplementary material Movie 2.

remaining polygonal meshwork, by a fluorescence recovery after photobleaching (FRAP) experiment, in which a patch was bleached and recovery of fluorescence within it was followed over time. As illustrated in Fig. 3 and supplementary material Movie 2, fluorescence in the bleached patch was recovered rapidly, and at the expense of another patch localised far away (~20 μm) in the same cell, demonstrating that in PDMP-treated cells the ER network is intact.

We next investigated the ultrastructure of the PDMP-induced ER domains. As shown in Fig. 4A, PDMP-treated cells contained well-defined patches of smooth membrane tubules (arrow) with lumens of similar calibre (~50 nm) to those of hepatic SER tubules. At high magnification, these patches were seen to consist of a convoluted network of tubules with frequent branching. A portion of a particularly convoluted patch, containing very thin tubules (<50 nm), is shown in Fig. 4B. When PDMP-treated cells were analysed by G-6-Pase EM cytochemistry, the cytochemical reaction product was present within the lumen of the tubules, again confirming their identity as ER subdomains (Fig. 4C). The ER membrane area:cytoplasmic volume ratio, estimated on images of cells treated for G-6-Pase cytochemistry, was not significantly different in PDMP-treated and untreated cells (Table 1).

We also analysed the effect of PDMP on the HeLa TetOff cells in which GFP-b(5)tail expression was kept repressed by doxycycline, and found that a much lower proportion (~10%) of treated cells exhibited the SER patches, revealed by calnexin staining (not shown). Moreover a quantitative analysis of cytoplasmic fluorescence intensity (FI) of induced cells containing or not containing SER patches in response to PDMP treatment revealed that the responding cells contained on average higher levels of GFP (average FI in arbitrary units of cells with patches 30.7±8.6 (s.d.) versus 20.6±5.3 in cells without patches (n=20); P=0.0005 by Student's t-test). Thus, expression of the construct and, presumably, the resulting expansion of the ER surface, increased the susceptibility of the ER to the action of PDMP.

To investigate whether SER patch induction is related to the GFP-b(5)tail construct or the cell line used in our experiments, we analysed the effect of PDMP on an MDCK cell line stably expressing an ER-restricted form of the integral membrane protein NADH-cytochrome b(5) reductase (b5R) (Borgese et al., 1996). PDMP also induced SER patches in a high proportion of cells in this line (supplementary material Fig. S1). By contrast, most of the parental MDCK cells failed to show ER restructuring in response to the drug, although a low percentage (<5%) did show small patches as revealed by staining for calnexin (supplementary material Fig. S1). Thus, the effect of PDMP is not restricted to one particular cell system.

PDMP-induced SER patches are dynamic and rapidly disperse upon removal of the drug

Live imaging of PDMP-treated cells revealed that the SER patches were dynamic (Fig. 5A and supplementary material Movie 1). Over minutes, they could be observed to fuse with each other (first three frames of top row of Fig. 5A), change shape and position (60-second versus 360-second frames of top row and 225-second versus 585-second frames of bottom row). Most remarkably, upon removal of PDMP, the patches were rapidly reabsorbed into the remaining polygonal meshwork (Fig. 5B and supplementary material Movie 3). Near complete dispersal of the structures was achieved in only 15 minutes, demonstrating the rapidity with which the ER can reorganise its structure.

ER components distribute differently between SER patches and polygonal meshwork ER

In cells in which RER and SER are spatially separated, ER proteins involved in the translocation and processing of nascent peptides are generally confined to the rough domains (Marcantonio et al., 1984; Meyer et al., 2000; Rolls et al., 2002; Vogel et al., 1990). Also reported to be more concentrated in the rough than in the smooth ER is CLIMP-63, a membrane protein that mediates the interaction between the ER and microtubules (Klopfenstein et al., 1998; Schweizer et al., 1995). To investigate whether rough ER proteins are partially or completely excluded from the PDMP-induced SER patches, we carried out confocal analyses of PDMP-treated cells. We first checked the accessibility of the SER patches to antibodies, by comparing the distribution of endogenous GFP fluorescence with that of GFP-b(5)tail revealed by indirect immunofluorescence, and found that the two patterns were superimposable (supplementary material Fig. S2A). We then compared the distribution of Sec61β (a translocon component) and CLIMP-63 with that of GFP-b(5)tail. As can be seen in Fig. 6 (second and third rows), both Sec61β and CLIMP-63 were less enriched in the SER patches than GFP-b(5)tail.

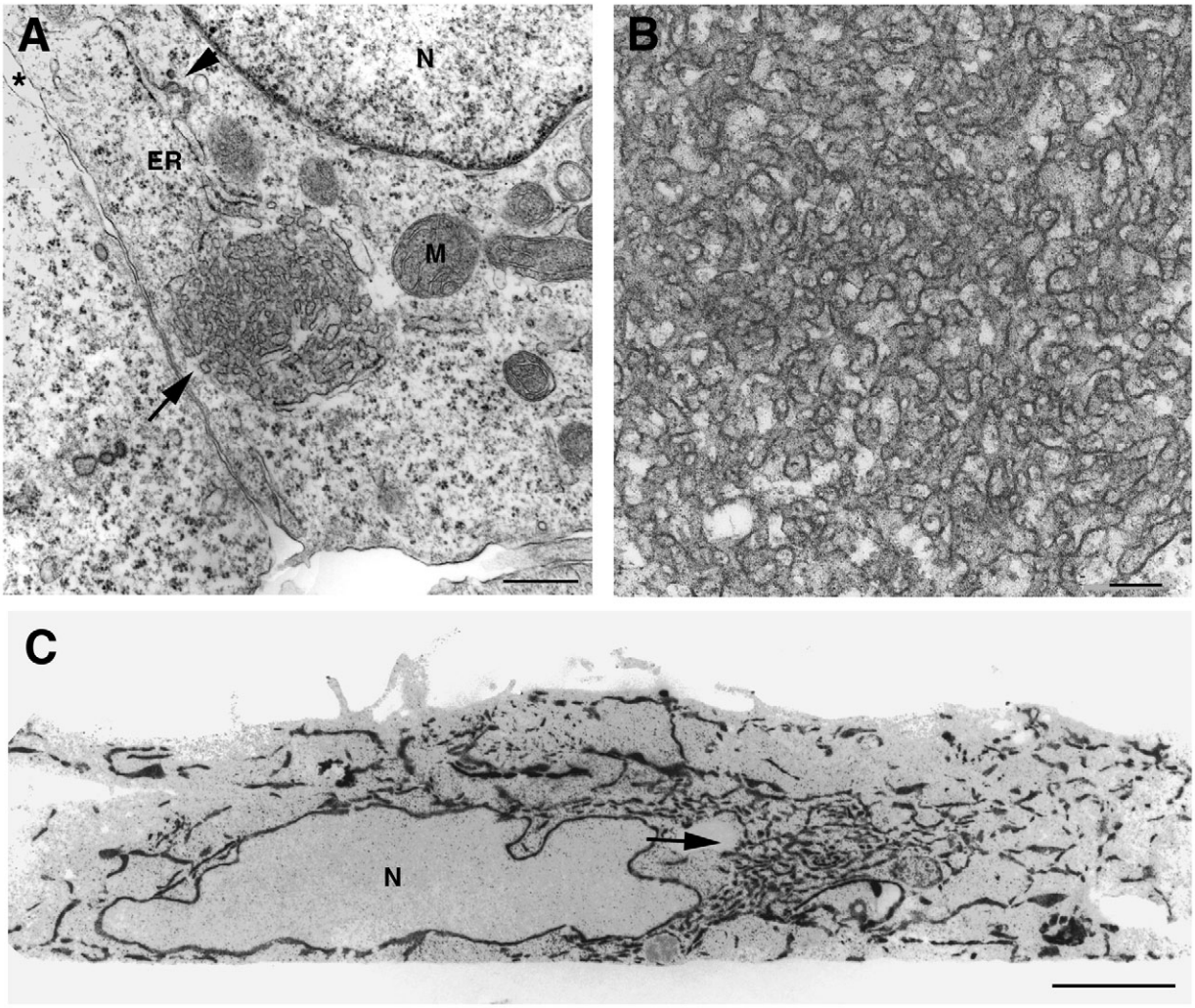

Fig. 4. Ultrastructure of PDMP-induced ER structures in induced HeLa TetOff cells. Conventional EM analysis at low (A) and high (B) magnification. (A) An SER patch is indicated by the arrow. Abundant free ribosomes are visible in the surrounding cytosol. The asterisk indicates the intercellular space. N, nucleus; M, mitochondrion; ER, elongated ER cisterna partly covered with ribosomes and containing a coated protrusion, which probably corresponds to an ER exit site (arrowhead). (B) A portion of a particularly convoluted SER patch consisting in a dense network of frequently branching tubules of small calibre. (C) G-6-Pase EM cytochemistry of a PDMP-treated cell. The arrow indicates an area of packed G-6-Pase-positive tubules that presumably corresponds to an SER patch. N, nucleus. Bars, 0.5 μm (A); 0.1 μm (B); 1 μm (C).

Strikingly, CLIMP-63 appeared to encircle the patches but was excluded from their interior. We also analysed the localisation within the patches of b5R, a membrane protein known to distribute both to SER and RER (Borgese and Pietrini, 1986), and of the lumenal protein calreticulin. As shown in Fig. 6 (top row), b5R, expressed after microinjection of the corresponding cDNA, appeared to be concentrated in the patches to a similar extent as GFP. Calreticulin was also concentrated in the patches (Fig. 6, last row), although there was some variability (see supplementary material Fig. S2A), which might be explained by different surface area to volume ratios in the different patches. COPII and ERGIC-53, (Schweizer et al., 1988), markers for exit sites and for the intermediate compartment, respectively, were also analysed (supplementary material Fig. S2B). COPII was excluded from the patches, whereas the recycling protein ERGIC-53 was present within them, but at variable concentration.

The results of Fig. 6 indicate that the PDMP-induced SER domains, like SER of tissues, differ from the RER in the relative concentrations of different ER proteins. We next asked whether there are also differences in the lipid composition of the SER patches compared with the rest of the ER. This question was addressed by investigating the distribution of microinjected carbocyanine lipid dyes. Carbocyanine dyes that contain saturated alkyl chains, like $DiIC_{18}(3)$ and $DiIC_{16}(3)$, are known to partition into liquid-ordered domains of the plasma membrane in living cells (Hao et al., 2001; Pierini et al., 1996; Thomas et al., 1994). When microinjected into different kinds of cells (Feng et al., 1994; Mehlmann et al., 1995; Terasaki and Jaffe, 1991; Terasaki et al., 1994) these dyes have been reported to stain the ER. Consistently, $DiIC_{16}(3)$ microinjected into induced HeLa cells, produced an ER staining pattern superimposable on that of GFP-b(5)tail (Fig. 7, upper row). After treatment with

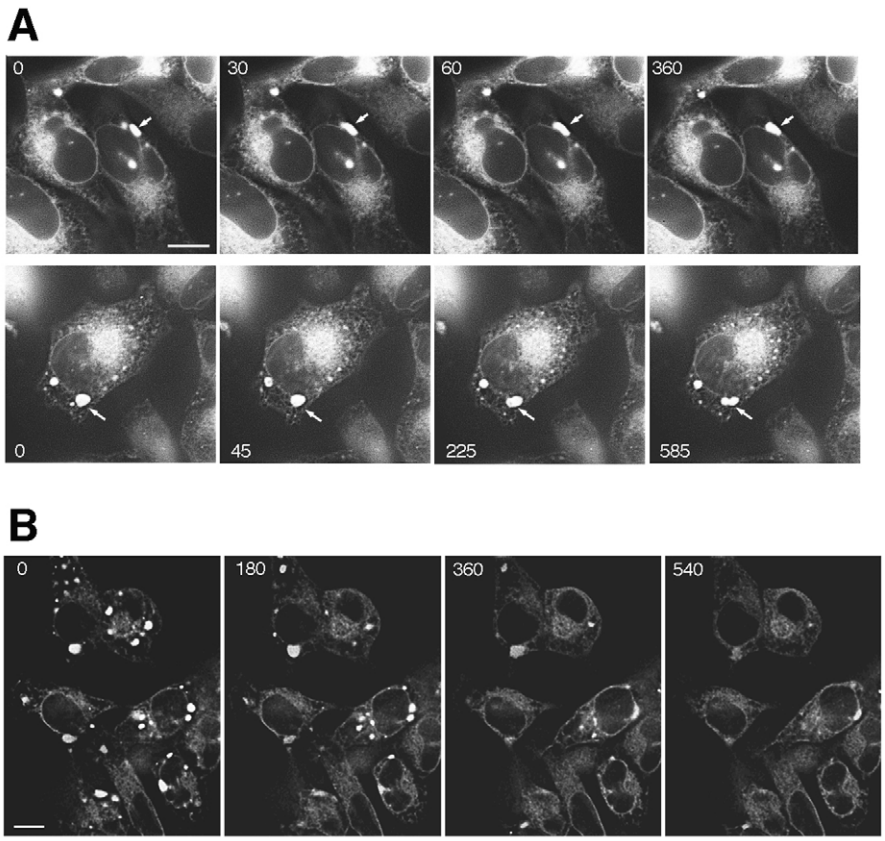

Fig. 5. SER patches are dynamic and are rapidly reabsorbed into the ER polygonal meshwork upon removal of PDMP. (A) Live imaging by wide-field microscopy of PDMP-treated HeLa TetOff cells. Each row shows a different field of cells, imaged in the presence of PDMP. The arrow in the top row images indicates an SER patch that has fused with a smaller one at 30 seconds. After 6 minutes the patch has become less elongated and has changed position relative to the nuclear envelope. The arrow in the bottom row indicates a large patch, which appears to be undergoing fission at the end of the imaging period. See Movie 1 in supplementary material for an illustration of the genesis and dynamics of SER patches. (B) PDMP-treated cells were placed in PDMP-free medium and immediately subjected to time-lapse imaging by wide-field microscopy. A movie of this sequence is available in supplementary material Movie 3). In all panels, the numbers on the left indicate the time (in seconds) from the start of the imaging experiment. Bars, 10 μm.

PDMP, the injected dye accumulated in the SER patches along with GFP-b(5)tail (Fig. 7, second row). We next investigated the distribution of a structural analogue of $DiIC_{18}(3)$, FAST-DiI, a dye containing unsaturated acyl chains, and reported to prefer liquid-disordered domains of the bilayer (Hao et al., 2001; Pierini et al., 1996). As shown in the third row of Fig. 7, FAST-DiI also diffused into a network that corresponded well with the GFP-b(5)tail-positive ER. However, in cells treated with PDMP, the fluorescence resulting from to the dye and the GFP-b(5)tail were no longer superimposable. As shown in the bottom row of Fig. 7, the FI in the SER patches relative to areas outside of the patches was weaker for FAST-DiI than for GFP. We quantified the ratio of FAST-DiI in the patches relative to the total cytoplasm (patches included) comparing it with the same ratio for GFP, and found that this ratio was 1.5±0.1 (s.d.) fold higher for GFP than for the lipid dye (P=3.4×10^{-5} in a paired t-test, n=6). When the same measurements were done for $DiIC_{16}(3)$ no significant difference between its distribution and that of GFP was revealed. These results suggest that not only proteins, but also lipids may be distributed differently between the SER patches and the remaining ER.

SER patches form by re-organisation of pre-existing smooth areas rather than by detachment of ribosomes

In principle, the formation of SER patches could be due to loss of ribosomes from the ER membrane or to a change in the architecture of pre-existing ribosome-free regions. We investigated whether PDMP caused detachment of ribosomes by isolating free ribosomes from the postnuclear supernatant (PNS) of GFP-b(5)tail-expressing cells treated or not with PDMP, and found that the percentage of RNA recovered in the free ribosome fraction was not significantly different in the two samples: 40% and 46.8% of the total RNA of the PNS was recovered in the free ribosomal pellet in untreated and PDMP treated cells, respectively.

We further confirmed by sucrose density gradient analysis that PDMP was not causing ribosome detachment (Fig. 8). In these experiments, we compared the density distribution of Sec61β and GFP-b(5)tail in PDMP-treated and untreated cells. In untreated cells, GFP-b(5)tail was present not only on Sec61β-bearing elements but also on vesicles of lower buoyant density, indicating that it is distributed to smooth portions of the ER, in which translocons are undetectable by this methodology (Fig. 8A). After PDMP treatment, the average buoyant density of Sec61β and of GFP-b(5)tail positive microsomes was not appreciably changed (1.163 and 1.133 with PDMP versus 1.160 and 1.135 without PDMP for Sec61β and of GFP-b(5)tail respectively), as would have been expected if ribosome detachment had occurred.

Mechanism of PDMP-induced changes in ER architecture

PDMP is best known for its ability to inhibit sphingolipid biosynthesis. At the concentrations of PDMP used in this study, both glycolipid and sphingomyelin synthesis are inhibited, with a resulting increase in intracellular ceramide concentration (Rosenwald et al., 1992). To investigate whether the effects of PDMP on ER architecture were due to accumulation of this sphingolipid, we pre-incubated cells with one of two drugs (β-chloro-L-alanine or Fumonisin B1) that interfere with ceramide biosynthesis. Each of the drugs was

then maintained in the medium during PDMP treatment. We found that neither drug had any detectable effect on PDMP-induced SER patch formation, suggesting that ceramide accumulation does not underlie this phenomenon (not shown). The dissociation of the effect of PDMP on ER architecture from its activity as sphingolipid synthesis inhibitor was further confirmed by the observation that the D (active) and L (inactive) isomers of the drug were both effective in inducing SER patches (data not shown).

In addition to inhibiting sphingolipid biosynthesis, PDMP has also been reported to interfere with Ca^{2+} homeostasis, causing release of the cation from the ER as well as inhibiting secondary Ca^{2+} influx from the extracellular medium, with a slightly elevated basal cytosolic Ca^{2+} concentration as end result (Kok et al., 1998). To investigate whether interference with Ca^{2+} homeostasis is involved in SER patch formation, we exposed PDMP-treated cells to the membrane-permeating Ca^{2+} chelator 1,2-bis(2-aminophenoxy)ethane-N,N,N′,N′-tetraacetic acid tetrakis(acetoxymethyl ester) (BAPTA-AM). As shown in Fig. 9, incubation with BAPTA-AM partially reversed the effect of PDMP. The percentage of cells showing SER patches, estimated from random images like those in Fig. 9, was reduced by nearly 50% in the BAPTA-AM-treated cells, and the difference was statistically highly significant. Thus, alterations in Ca^{2+} homeostasis may at least partially explain the effect of PDMP on ER organisation.

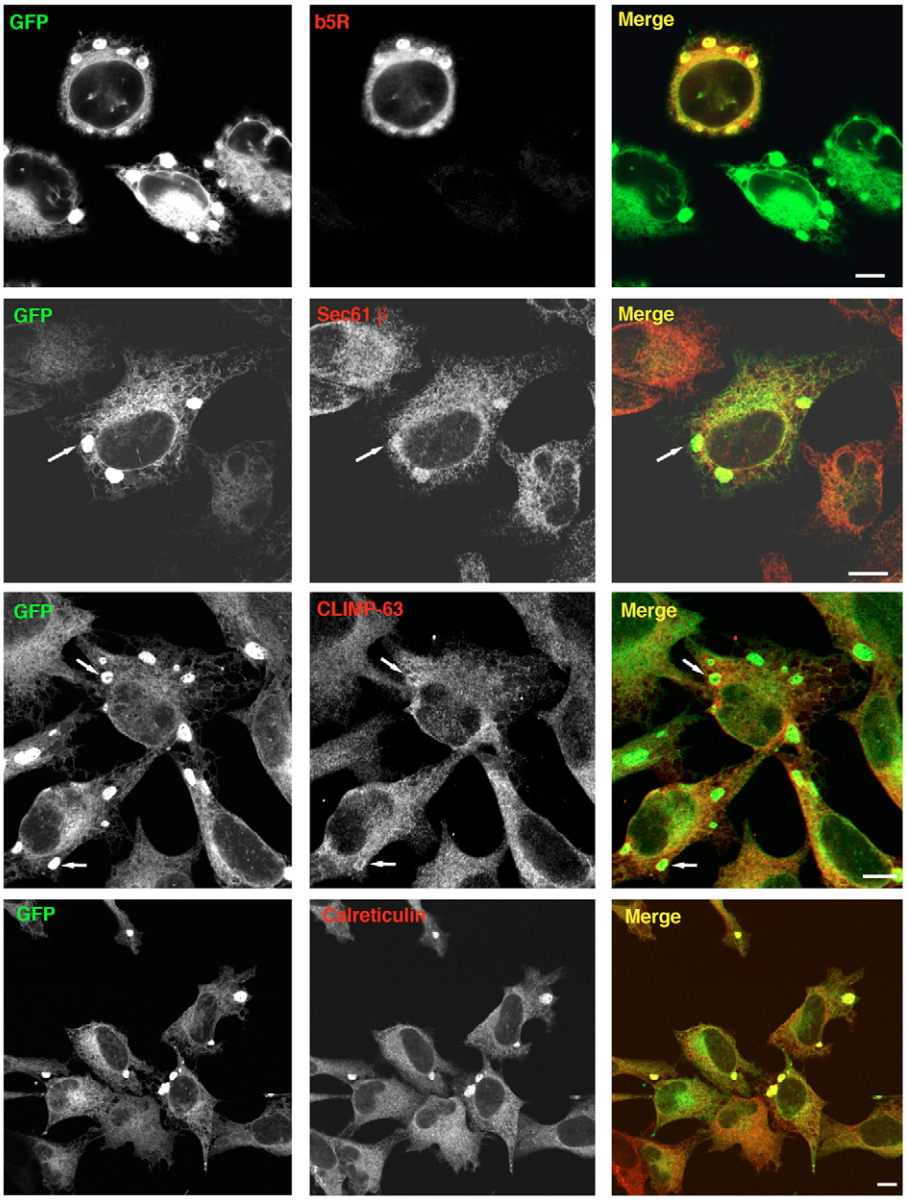

Fig. 6. Distribution of ER proteins between SER patches and polygonal meshwork ER. (Top row) HeLa TetOff cells expressing GFP-b(5)tail and microinjected with a plasmid coding for G2A b5R were treated with PDMP and immunostained for b5R. Three bottom rows: PDMP-treated cells were immunostained for Sec61β (second row), CLIMP-63 (third row) or calreticulin (bottom row), with the use of Alexa Fluor 568-conjugated secondary antibodies. The cells were then analysed by confocal microscopy. The arrows in the Sec61β and CLIMP-63 panels indicate evident SER patches with low content of the two RER markers. Note the tendency of CLIMP-63 to encircle the SER patches. Bars, 10 μm.

Discussion

In order to be contained within a limited cytoplasmic volume, the large surface area of the ER membrane (Weibel et al., 1969) must necessarily be folded into tubular or lamellar structures, generating a complex architecture that varies in response to the functional requirements of different cell types or conditions. A common type of ER organisation is the SER random tubular network that is segregated from RER domains. SER is generated when the ER surface area required to house a subset of resident membrane proteins exceeds that needed for ER-associated protein synthesis, but the mechanisms of its segregation from RER have been unclear.

The SER random tubular network expands rapidly in response to the synthesis of many ER membrane proteins. For instance, in hepatocytes, its extension increases dramatically after exposure of the cells to xenobiotics that induce the synthesis of ER-resident enzymes involved in drug metabolism (Orrenius and Ericsson, 1966). Overexpression of ER-resident membrane proteins can also induce SER random tubular network formation in cells in which it is normally not detected, such as in cultured cells, which generate this compartment in response to overexpression of a variety of ER-resident wild-type or mutated proteins (Jingami et al., 1987; Sandig et al., 1999; Snapp et al., 2003).

In all the examples above, formation of random tubular SER is inextricably linked to membrane proliferation. In the present

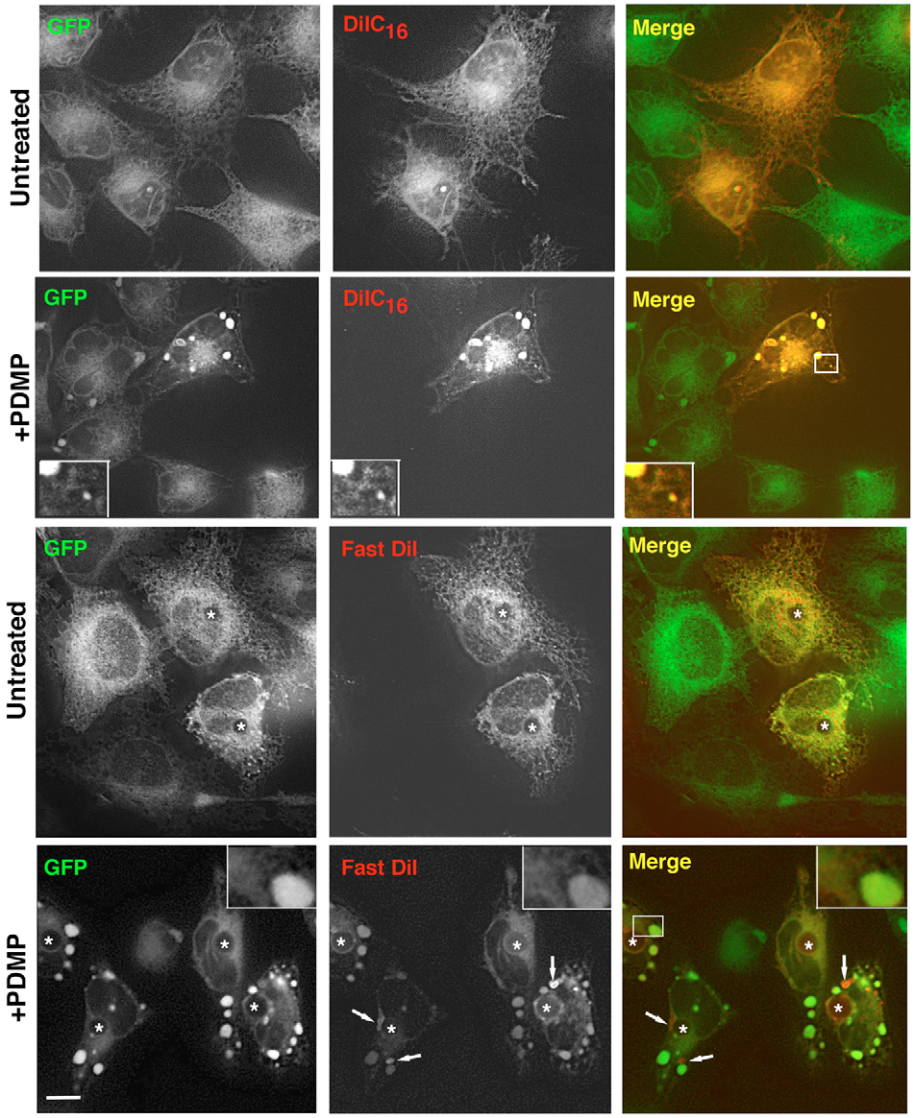

Fig. 7. Distribution of lipid dyes between SER patches and polygonal meshwork ER. Induced HeLa TetOff were microinjected with $DiIC_{16}$(3) (two upper rows) or with FAST-DiI (two lower rows) dissolved in soybean oil. One set of cells was then exposed to PDMP whereas another set was exposed to the vector, as indicated to the left of the figure. Live cells were imaged by wide-field microscopy 3 hours later. The asterisks are placed at the centre of the microinjected oil droplets. Note in the bottom row (inset) the prevalence of the GFP fluorescence in the PDMP-induced patches compared with FAST-DiI. The boxes in the right panel of the second and fourth rows indicate areas that are enlarged (threefold) in the insets. The arrows in the bottom row indicate uncharacterised structures in which FAST-DiI is particularly concentrated. Bar, 10 μm.

work, we describe a cell model in which the drug PDMP induces the rearrangement of a pre-existing ER polygonal meshwork, with the reversible segregation of random tubular SER domains in the absence of membrane proliferation. These results illustrate the dynamic nature of the relation between rough and smooth regions of the ER.

The SER patches were induced by PDMP in HeLa cells inducibly expressing an ER-targeted tail-anchored GFP [GFP-b(5)tail], and rapidly disappeared after removal of the drug. By EM, the patches resembled the SER of tissues as well as the ER clumps observed in the vegetal cortex of maturing *Xenopus* oocytes (Terasaki et al., 2001). The resemblance of the PDMP-induced patches to physiological SER was not limited to morphology, but also involved the differential distribution within them of smooth and RER proteins, as assessed by immunofluorescence. The high FI of GFP-b(5)tail within the patches could probably be largely accounted for by the density of membrane packing in these structures, so that the surface concentration of the construct was probably the same in patch and polygonal meshwork membranes. Thus, the lower relative concentration of Sec61β and CLIMP-63 in the SER patches suggests a preferential localisation of the two proteins to ER domains outside these domains. In any case, the different distribution of the two RER proteins with respect not only to the GFP-b(5)tail, but also to a general ER membrane marker, b5R, as well as to a lumenal protein, indicates that the protein composition of the SER patches differs from that of the remaining polygonal meshwork.

Interestingly, the experiments with lipid dyes suggest that the SER patches also differed from the remaining ER in lipid composition. Whereas the dye $DiIC_{16}$(3), known to partition into liquid-ordered domains of the plasma membrane in living cells (Hao et al., 2001; Pierini et al., 1996; Thomas et al., 1994), was distributed between SER patches and polygonal meshwork ER in a manner indistinguishable from GFP-b(5)tail, the dye FAST-DiI, which partitions preferentially into fluid bilayer domains (Hao et al., 2001; Pierini et al., 1996), was less enriched in the patches, suggesting that they could have a higher degree of rigidity than the remaining ER. Consistent with this idea, one publication (Colbeau et al., 1971) reported that phospholipids of hepatic smooth microsomes have a higher proportion of saturated acyl chains

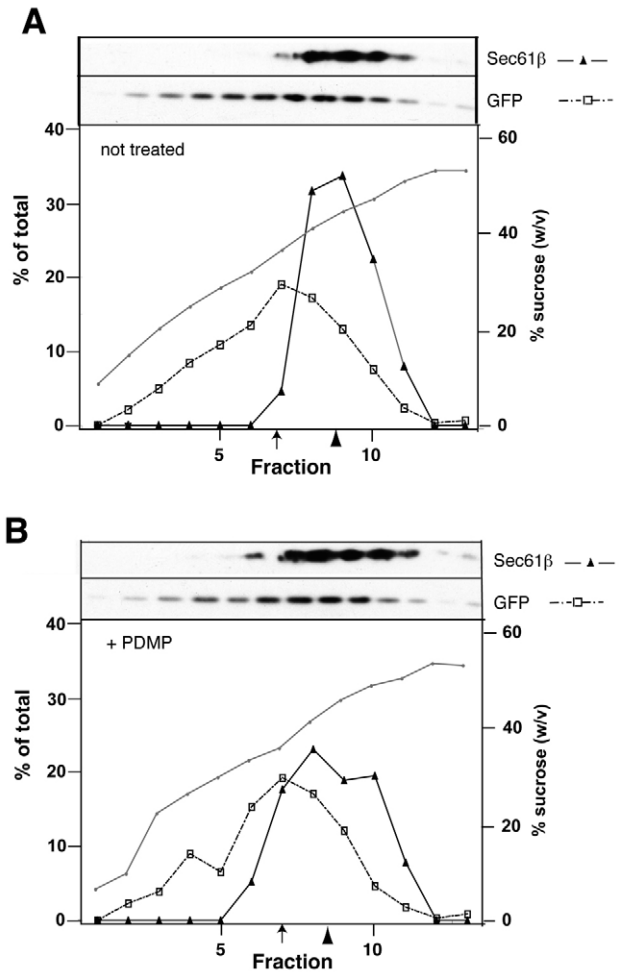

Fig. 8. Sucrose density gradient analysis of PDMP-treated and untreated cells. PNS obtained from total homogenates of induced untreated (A) or PDMP-treated (B) HeLa TetOff cells were centrifuged on sucrose density gradients. An equal aliquot of each fraction was analysed by western blotting for Sec61β and GFP-b(5)tail, as indicated. The grey line in both panels indicates the percentage of sucrose in each fraction, determined gravimetrically. The arrow and arrowhead below the abscissa indicate the average sucrose concentration at which elements containing GFP-b(5)tail (arrow) and Sec61β (arrowhead) equilibrate.

than those of rough microsomes. However, the interpretation of these data is complicated by the unavoidable problem of cross-contamination between subcellular fractions in biochemical experiments.

The PDMP-induced restructuring of the ER that we report here has not been previously observed by others, and indeed we noted a less-marked effect of the drug on untransfected TetOff cells or on transfected cells in which GFP-b(5)tail expression was repressed by doxycycline. However, the effect of the drug was not due to particular properties of the GFP-b(5)tail construct nor to the HeLa cell line we used, because ER patches were also observed in MDCK cells overexpressing another ER membrane protein (b5R). The increased susceptibility to PDMP of the ER of cells overexpressing resident membrane proteins is probably related to membrane proliferation, a phenomenon that we demonstrated here for the GFP-b(5)tail, and that is caused also by other ER membrane proteins (Federovitch et al., 2005). Thus, PDMP presumably can exert its effect only on an ER substrate containing enough 'extra' smooth membrane, as provided by the induced HeLa TetOff cells. Consistently, we found no evidence that PDMP detaches ribosomes from ER membranes, indicating that the drug was inducing a reorganisation of pre-existing smooth membranes.

The factors determining ER organisation are still debated and are the object of intense investigation. The available data suggest that the architecture of the organelle is determined both by intrinsic factors (proteins and/or lipids) of the ER membrane itself and by the interaction of the membranes with the microtubule cytoskeleton. Thus, although microsomal vesicles can assemble into a branching tubular network in the absence of microtubules (Dreier and Rapoport, 2000; Paiement et al., 1990) and even in the absence of any cytosolic factor (Voeltz et al., 2006) the distribution of tubules, their extension and the regulation of their branching is microtubule dependent (Dabora and Sheetz, 1988; Lee and Chen, 1988; Terasaki et al., 1986; Waterman-Storer and Salmon, 1998). The SER random tubular

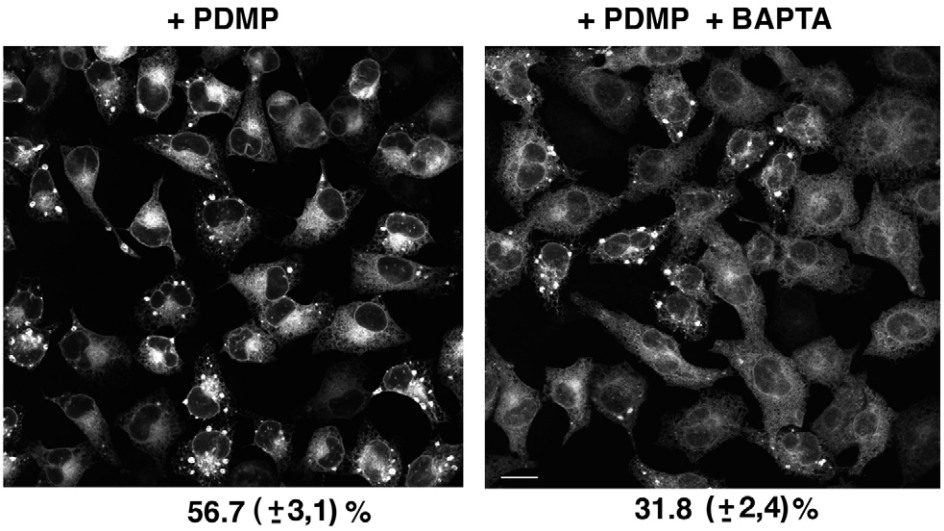

Fig. 9. Intracellular Ca^{2+} chelation partially reverses the effect of PDMP on ER architecture. Induced HeLa TetOff cells were treated with 100 μM PDMP for 3 hours. During the last hour of incubation the medium was supplemented with 50 μM BAPTA-AM (right panel) or vector (left panel). After fixation, the cells were analysed by confocal microscopy. The percentage of cells showing SER patches was determined on eight randomly selected fields, such as those illustrated in the figure. The difference between the percentages of responding cells under the two conditions (indicated under the panels ± s.e.m.) was highly significant by Student's *t*-test ($P=1.7\times10^{-5}$).

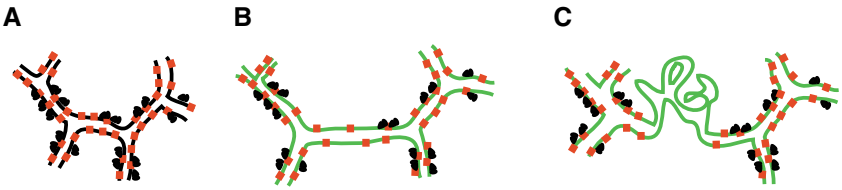

Fig. 10. Model of SER patch formation. (A) In HeLa cells not expressing GFP-b(5) tail, ribosome-free and ribosome-covered areas are interspersed along the same tubules. A protein or protein complex (red squares) is responsible for maintaining relatively straight tubules and for regulating the branching frequency. (B) GFP-b(5)tail expression induces an increase in ER surface area without a concomitant increase in the expression of ER membrane proteins. This results in dilution of the protein complex that regulates tubule geometry. (C) Minor perturbations induced by PDMP cause the regulatory protein(s) to cluster with ribosomes, leaving large areas of ER free to collapse into a random tubular network. See text for further explanation.

network is characterised by highly convoluted tubules rather than by the relatively straight ones of the polygonal meshwork and could thus represent a spontaneous arrangement of the ER – similar to the so-called 'sponge phase' of curvature theoreticians (Hyde et al., 1997) – that is attained in the absence of regulatory factors mediating interaction with microtubules. Consistently, CLIMP-63, a membrane protein that mediates static interaction of the RER with microtubules (Farah et al., 2005; Klopfenstein et al., 1998; Schweizer et al., 1995) was excluded from the interior of the SER patches.

On the basis of the considerations above, we propose a model for the PDMP-induced formation of SER patches, illustrated in Fig. 10. Under normal conditions (Fig. 10A), a dynamic polygonal meshwork is maintained thanks to the presence of ER organising membrane proteins (red squares) that are required, with the cooperation of the cytoskeleton, to stretch the tubules and regulate their branching. Upon overexpression of GFP-b(5)tail (Fig. 10B), the ER membrane (now pictured in green) expands without a concomitant increase in the amount of other ER membrane proteins. [Indeed, we found that the amount of ribophorin I and Sec61β in our HeLa TetOff cells was not increased after induction of GFP-b(5)tail expression (data not shown).] This leads to a dilution of the organising proteins. Nonetheless, under normal conditions, their concentration remains sufficient to maintain the ER polygonal meshwork architecture. Small perturbations, however, lead to clustering of the organising proteins (Fig. 10C) that now roughly regain the surface density that they had in uninduced cells (Fig. 10A). The resulting ample areas of ER lacking the organising proteins then collapse into a random tubular network. The exclusion of ribosomes from the SER patches could be explained either by an association of the organising proteins with components of the translocation apparatus or, more simply, by the unsuitability of the geometry of the random tubular network to serve as platform for polysomes. Engaged translocon complexes diffuse very slowly in the ER membrane, but their diffusion rate increases when protein synthesis is stopped (Nikonov et al., 2002). Thus, engaged translocons would be trapped in the polygonal meshwork, while free translocons could diffuse in and out of the SER patches, explaining the presence in these structures of some Sec61β, detected by immunofluorescence. Finally, one can imagine that in situations where the ER membrane surface extension is higher and the organising proteins become more diluted than pictured in Fig. 10B, random tubular network SER will also segregate from the polygonal meshwork in the absence of a perturbing agent like PDMP.

In this study, we initially used PDMP because it is a known inhibitor of sphingolipid synthesis. However, we found that the effect of the drug on ER structure was not related to this activity. Rather, our results suggest that the induction of SER patches may in part be due to perturbation of Ca^{2+} homeostasis, a second effect of the drug (Kok et al., 1998). Indeed, treatment of cells with the Ca^{2+} chelator BAPTA-AM partially reversed the effect of PDMP. Increases in cytosolic [Ca^{2+}] induced by ionomycin have previously been reported to cause restructuring of the ER (Dreier and Rapoport, 2000; Pedrosa Ribeiro et al., 2000; Subramanian and Meyer, 1997), however, the high cytosolic Ca^{2+} concentration attained in these experiments appeared to cause fragmentation of the network (Subramanian and Meyer, 1997). By contrast, under our conditions, connectivity of the ER was maintained, as demonstrated by FRAP experiments. The basis for the dependency of ER structure on Ca^{2+} homeostasis is presently unclear, and multiple molecular interactions may be involved. In this context, it is worth mentioning that one protein mediating static interaction between the ER and microtubules, p22, is Ca^{2+} dependent (Andrade et al., 2004).

In conclusion, our study reveals a dynamic and reversible segregation between rough and smooth domains of the ER, which we believe has important implications for the mechanisms that govern ER architecture in tissues. The system we describe here may provide a useful tool for the further study of the molecular basis of ER organisation.

Materials and Methods

Antibodies

Polyclonal antibodies against GFP were from MBL International Corporation; polyclonal IgG against calnexin, giantin, Sec61β, CLIMP63, and calreticulin were kind gifts of A. Helenius (ETH, Zuerich, CH), M. Renz (Institute for Immunology and Molecular Genetics, Karlsruhe, Germany), Ramanujan S. Hegde (N.I.H, Bethesda, MD) (Snapp et al., 2003), H.-P. Hauri (Biozentrum, University of Basel, Switzerland) and Marek Michalak (University of Edmonton, Canada), respectively. Anti-cytochrome b5 reductase (b5R) antiserum has been described in previous studies (Colombo et al., 2005). Secondary, peroxidase-conjugated anti-rabbit IgG (used for western blotting) was from Pierce; Alexa Fluor 568- and Texas Red-conjugated anti-rabbit or anti-mouse IgGs were from Molecular Probes, and Jackson Immunoresearch, respectively.

Plasmid construction, transfection and selection of HeLa TetOff lines expressing GFP-b(5)tail

A cDNA coding for the construct GFP-b(5) tail was subcloned under the Tet responsive element of the plasmid pTRE from Clontech. The cDNA codes for enhanced GFP (EGFP from Clontech) joined through a linker sequence to the tail region of cyt b(5) (Snapp et al., 2003) and is described in detail in (Bulbarelli et al., 2002) with the name GFP-17. The cDNA was excised with *Hin*dIII and *Xba*I from pcDNA3 (Invitrogen). After filling with Klenow, the fragment was cloned into the filled *Eco*RI site of pTRE. A plasmid encoding an ER-restricted form of b5R (G2A mutant) under the cytomegalovirus promoter has been described (Borgese et al., 1996).

HeLa TetOff cells (from Clontech), grown in DMEM supplemented with 100 μg/ml G418, streptomycin, penicillin and 10% Tet-approved fetal bovine serum (Clontech) at 37°C under a 5% CO_2 atmosphere, were co-transfected with pTRE-GFP-b(5)tail and pTK-Hygr plasmid (Clontech). G418- and hygromycin-resistant clones were selected and maintained in culture in the presence of doxycycline (0.1 μg/ml). To induce expression of GFP-b(5)tail, the cells were plated in doxycycline-

free medium. The medium was replaced 1 day after plating and cells were usually analysed 2-3 days thereafter.

Drug treatments

Cells were treated for 2-3 hours with 50-100 μM (±) threo-PDMP (Sigma) or the D- or L-optical isomer of the same compound (Matreya) diluted from a 100 mM stock solution in ethanol. In some experiments, 50 μM BAPTA-AM (Sigma), diluted from a 25 mM stock solution in dimethylsulfoxide, was added during the last hour of incubation. β-chloro-L-alanine and Fumonisin B1 (both from Sigma) were dissolved in PBS and used at 2 mM and 0.1 mM, respectively. In all experiments, control incubations were carried out with equal volumes of drug-free vector.

Microinjection

Lipid dyes

25 μl of soybean oil were added to 250 μg of FAST-DiI or $DiIC_{16}(3)$ (Molecular Probes) and the suspension was incubated at 45°C for 1 hour with intermittent vortexing to allow dissolution of the dye. The resulting solution was centrifuged three times at 13,800 $\boldsymbol{g}_{max}$ for 15 minutes, and the final supernatant was microinjected into HeLa cells with the use of an Eppendorf 5200 microinjector. A pressure of ~5000 hPa (the cleaning pressure) was applied, which resulted in the deposition of a 5-10 μm oil droplet inside the cell. After microinjection, cells were incubated with or without PDMP for 3 hours and then imaged.

G2A b5R plasmid

A 1 μg/μl solution of the plasmid was microinjected into induced cells applying a pressure of 80-100 hPa. 75 minutes after microinjection the cells were treated for 3 hours with PDMP and then fixed and analysed.

Immunofluorescence and live-cell imaging

Cells grown on coverslips were processed for immunofluorescence either by our standard protocol (De Silvestris et al., 1995) or by a modified procedure that includes treatment of the fixed cells with RNase A to improve accessibility of translocon-associated components (Snapp et al., 2004). Immunofluorescent specimens were observed under a Nikon eclipse E600 microscope attached to a Bio-Rad MRC 1024 ES confocal system, with the use of 60× or 40× oil-immersion objectives. In doubly fluorescent images, acquisition was always in the sequential mode, and merged images were constructed from the single acquisitions with the aid of Adobe Photoshop software. In all figures, the single acquisitions are shown in greyscale, and the merged image in RGB colour. All images show single confocal sections, unless otherwise specified.

For the FRAP experiment reported in Fig. 4, the coverslip containing adherent cells was mounted on a microscope slide with a chamber containing PBS + Ca^{2+} and Mg^{2+} (1 mM each) and 100 μM PDMP at room temperature. Areas of GFP-b(5)tail-expressing cells were bleached by bringing the optical zoom to 10 and scanning the zoomed area 20 times with full laser power. The zoom was then returned to 1 and images were acquired in time lapse with the laser power set at 3%.

Other live-cell imaging was carried out with a Zeiss Axiovert 200M inverted microscope equipped with temperature (set at 37°C) and CO_2 concentration (set at 5%) controllers, and a Roper MicroMax CCD 512×512 camera controlled by MetaMorph program (Crisel Instruments, Rome). The 63× oil-immersion PlanApochromat (NA) objective was used. 2D deconvolution of images was carried out with the Huygens Essential programme from Scientific Volume Imaging (Hilversum, the Netherlands).

FI of cytoplasmic areas were determined with the aid of Metamorph software. The FI of images to be used for quantitative determinations was always kept below saturation and no contrasting was applied.

EM and glucose-6-phosphatase cytochemistry

Conventional EM was carried out according to standard procedures (Snapp et al., 2003). Cytochemical detection of G-6-Pase activity was performed as described by Griffiths et al. (Griffiths et al., 1983), modified by Celli et al. (Celli et al., 2003), except that the enzyme reaction was carried out with 1%, instead of 0.1%, (wt/vol) lead nitrate in 80 mM Tris-maleate buffer pH 6.5.

Morphometry

Surface area normalised to cytoplasmic volume was measured on electron micrographs of randomly selected cells (with a constant magnification of 16,500×) as described (Griffiths, 1993). Briefly, a grid with 1×1 cm squares was randomly superimposed on the photos, and the surface area of ER elements was estimated by counting the number of intersections between G-6-Pase-positive profiles and the grid lines (intersection counts); the volume of the cytoplasm was estimated by counting the number of intersections of the grid lines themselves that fell within the cell, excluding the nucleus (point counts). The intersection to point ratio was considered as a measure of the ER surface area density.

Cell fractionation

Sucrose density gradient centrifugation

Approximately 3.5×10^6 cells expressing GFP-b(5)tail, treated or not with PDMP, were collected from a 150 mm Petri dish and washed and resuspended with 0.6 ml of an ice-cold homogenisation buffer consisting of 20 mM HEPES-K^+, pH 7.3, 120 mM sucrose and a protease inhibitor cocktail (Bulbarelli et al., 2002). All subsequent operations were carried out at 0-4°C. Cells were ruptured by 30-40 passages through a cell cracker (0.0013 inch clearance), and the resulting homogenates were collected in a total volume of 0.9 ml of homogenisation buffer. After elimination of nuclei by centrifugation at 800 $\boldsymbol{g}_{max}$ for 10 minutes, 0.6 ml of the PNS were loaded on sucrose gradients composed of successive 0.5 ml layers containing 20, 25, 30, 35, 40, 45, 50, 55 and 60% sucrose, all in 20 mM HEPES-K^+, pH 7.3. The gradients were centrifuged at 304,000 $\boldsymbol{g}_{max}$ for 75 minutes in an SW 55 Ti rotor (Beckman), and 13 fractions of 0.4 ml were then collected from the top.

Isolation of free ribosomes

Cells expressing GFP-b(5)tail, were grown to ~70% confluence in 100 mm Petri dishes. Four dishes were treated with 100 μM PDMP and four were left untreated. Subsequent steps were carried out in the cold. All solutions (except the ones in the final step gradient) contained either 0.1 mM PDMP or an equivalent volume of ethanol. The cells were washed with PBS and then resuspended in 400 μl of a hypotonic buffer (1 mM Tris-HCl, pH 7.4, 15 mM KCl, 0.1 mM EDTA plus protease inhibitors). The cells were allowed to swell for 5 minutes, and then supplemented with 400 μl of a compensating buffer (to re-establish isotonicity) containing 0.5 M sucrose plus the same components as the hypotonic buffer. The cells were then ruptured in a cell cracker, the homogenate was brought to 2 ml with isotonic buffer, and nuclei were eliminated by centrifugation as in the previous paragraph. The PNS was adjusted to contain 25 mM KCl, 0.5 mM $MgCl_2$ and 10 mM Tris-HCl, pH 7.5 (TKM) and layered over a discontinuous gradient consisting of two 0.75 ml layers of 2.0 and 0.8 M sucrose, containing TKM. The gradients were centrifuged for 17 hours at 195,000 $\boldsymbol{g}_{max}$ in a TLA 100.3 rotor (Beckman). The pellet, containing the free ribosomes, was redissolved in a small volume of 0.25 M sucrose-TKM.

Biochemical assays

Protein was determined by the Bradford assay (reagents from Pierce), and RNA as described (Munro and Fleck, 1966). SDS-PAGE and western blotting were carried out as detailed in previous publications (Bulbarelli et al., 2002). Western blots were developed with SuperSignal® West Pico or Dura Chemiluminescent Substrate from Pierce.

In addition to the people who kindly donated antibodies, listed in the Materials and Methods section, we thank Pietro De Camilli for critically reading the manuscript, Silvia Brambillasca and Sara Colombo for their helpfulness in the lab, and Francesca Lombardo for collaboration in the EM studies. This work was partially supported by CNR grant ME-P02-IN-C2-M001 to the Institute for Neuroscience, and by a grant from the Italian Ministry of Research PRIN-COFIN to N.B.

References

Anderson, R. G., Orci, L., Brown, M. S., Garcia-Segura, L. M. and Goldstein, J. L. (1983). Ultrastructural analysis of crystalloid endoplasmic reticulum in UT-1 cells and its disappearance in response to cholesterol. *J. Cell Sci.* **63**, 1-20.

Andrade, J., Zhao, H., Titus, B., Timm Pearce, S. and Barroso, M. (2004). The EF-hand Ca2+-binding protein p22 plays a role in microtubule and endoplasmic reticulum organization and dynamics with distinct Ca2+-binding requirements. *Mol. Biol. Cell* **15**, 481-496.

Borgese, N. and Pietrini, G. (1986). Distribution of the integral membrane protein NADH-cytochrome b_5 reductase in rat liver cells, studied with a quantitative radioimmunoblotting assay. *Biochem. J.* **239**, 393-403.

Borgese, N., Aggujaro, D., Carrera, P., Pietrini, G. and Bassetti, M. (1996). A role for N-myristoylation in protein targeting: NADH-cytochrome b_5 reductase requires myristic acid for association with outer mitochondrial but not endoplasmic reticulum membranes. *J. Cell Biol.* **135**, 1501-1513.

Bulbarelli, A., Sprocati, T., Barberi, M., Pedrazzini, E. and Borgese, N. (2002). Trafficking of tail-anchored proteins: transport from the endoplasmic reticulum to the plasma membrane and sorting between surface domains in polarised epithelial cells. *J. Cell Sci.* **115**, 1689-1702.

Celli, J., de Chastellier, C., Franchini, D. M., Pizarro-Cerda, J., Moreno, E. and Gorvel, J. P. (2003). Brucella evades macrophage killing via VirB-dependent sustained interactions with the endoplasmic reticulum. *J. Exp. Med.* **198**, 545-556.

Colbeau, A., Nachbaur, J. and Vignais, P. M. (1971). Enzyme characterization and lipid composition of rat liver subcellular membranes. *Biochem. Biophys. Acta* **249**, 462-492.

Colombo, S., Longhi, R., Alcaro, S., Ortuso, F., Sprocati, T., Flora, A. and Borgese, N. (2005). N-myristoylation determines dual targeting of mammalian NADH-cytochrome b5 reductase to ER and mitochondrial outer membranes by a mechanism of kinetic partitioning. *J. Cell Biol.* **168**, 735-745.

Dabora, S. L. and Sheetz, M. P. (1988). The microtubule-dependent formation of a tubulovesicular network with characteristics of the ER from cultured cell extracts. *Cell* **54**, 27-35.

De Matteis, M. A., Luna, A., Di Tullio, G., Corda, D., Kok, J. W., Luini, A. and Egea, G. (1999). PDMP blocks the BFA-induced ADP-ribosylation of BARS-50 in isolated Golgi membranes. *FEBS Lett.* **459**, 310-312.

De Silvestris, M., D'Arrigo, A. and Borgese, N. (1995). The targeting information of the mitochondrial outer membrane isoform of cytochrome b_5 is contained within the carboxyl-terminal region. *FEBS Lett.* **370**, 69-74.

Dreier, L. and Rapoport, T. A. (2000). In vitro formation of the endoplasmic reticulum occurs independently of microtubules by a controlled fusion reaction. *J. Cell Biol.* **148**, 883-898.

Farah, C. A., Liazoghli, D., Perreault, S., Desjardins, M., Guimont, A., Anton, A., Lauzon, M., Kreibich, G., Paiement, J. and Leclerc, N. (2005). Interaction of microtubule-associated protein-2 and p63: a new link between microtubules and rough endoplasmic reticulum membranes in neurons. *J. Biol. Chem.* **280**, 9439-9449.

Farsad, K. and De Camilli, P. (2003). Mechanisms of membrane deformation. *Curr. Opin. Cell Biol.* **15**, 372-381.

Fawcett, D. W. (1981). *The Cell*. Philadelphia: W. B. Saunders.

Federovitch, C. M., Ron, D. and Hampton, R. Y. (2005). The dynamic ER: experimental approaches and current questions. *Curr. Opin. Cell Biol.* **17**, 409-414.

Feng, J. J., Carson, J. H., Morgan, F., Walz, B. and Fein, A. (1994). Three-dimensional organization of endoplasmic reticulum in the ventral photoreceptors of Limulus. *J. Comp. Neurol.* **341**, 172-183.

Futerman, A. H. and Riezman, H. (2005). The ins and outs of sphingolipid synthesis. *Trends Cell. Biol.* **15**, 312-318.

Gossen, M. and Bujard, H. (1992). Tight control of gene expression in mammalian cells by tetracycline-responsive promoters. *Proc. Natl. Acad. Sci. USA* **89**, 5547-5551.

Griffiths, G. (1993). Fine structure immunocytochemistry. Heidelberg, NewYork, London, Paris: Springer-Verlag.

Griffiths, G., Quinn, P. and Warren, G. (1983). Dissection of the Golgi complex. I. Monensin inhibits the transport of viral membrane proteins from medial to trans Golgi cisternae in baby hamster kidney cells infected with Semliki Forest virus. *J. Cell Biol.* **96**, 835-850.

Griner, R. D. and Bollag, W. B. (2000). Inhibition of [(3)H]thymidine transport is a nonspecific effect of PDMP in primary cultures of mouse epidermal keratinocytes. *J. Pharmacol. Exp. Ther.* **294**, 1219-1224.

Hao, M., Mukherjee, S. and Maxfield, F. R. (2001). Cholesterol depletion induces large scale domain segregation in living cell membranes. *Proc. Natl. Acad. Sci. USA* **98**, 13072-13077.

Hyde, S., Andersson, S., Larsson, K., Blum, Z., Landh, T., Lidin, S. and Ninham, B. W. (1997). *The Language of Shape. The Role of Curvature in Condensed Matter: Physics, Chemistry and Biology*. Amsterdam: Elsevier.

Jingami, H., Brown, M. S., Goldstein, J. L., Anderson, R. G. and Luskey, K. L. (1987). Partial deletion of membrane-bound domain of 3-hydroxy-3-methylglutaryl coenzyme A reductase eliminates sterol-enhanced degradation and prevents formation of crystalloid endoplasmic reticulum. *J. Cell Biol.* **104**, 1693-1704.

Kepes, F., Rambourg, A. and Satiat-Jeunemaitre, B. (2005). Morphodynamics of the secretory pathway. *Int. Rev. Cytol.* **242**, 55-120.

Klopfenstein, D. R., Kappeler, F. and Hauri, H. P. (1998). A novel direct interaction of endoplasmic reticulum with microtubules. *EMBO J.* **17**, 6168-6177.

Kok, J. W., Babia, T., Filipeanu, C. M., Nelemans, A., Egea, G. and Hoekstra, D. (1998). PDMP blocks brefeldin A-induced retrograde membrane transport from golgi to ER: evidence for involvement of calcium homeostasis and dissociation from sphingolipid metabolism. *J. Cell Biol.* **142**, 25-38.

Lee, C. and Chen, L. B. (1988). Dynamic behavior of endoplasmic reticulum in living cells. *Cell* **54**, 37-46.

Maceyka, M. and Machamer, C. E. (1997). Ceramide accumulation uncovers a cycling pathway for the cis-Golgi network marker, infectious bronchitis virus M protein. *J. Cell Biol.* **139**, 1411-1418.

Marcantonio, E. E., Amar-Costesec, A. and Kreibich, G. (1984). Segregation of the polypeptide translocation apparatus to regions of the endoplasmic reticulum containing ribophorins and ribosomes. II. Rat liver microsomal subfractions contain equimolar amounts of ribophorins and ribosomes. *J. Cell Biol.* **99**, 2254-2259.

McMahon, H. T. and Gallop, J. L. (2005). Membrane curvature and mechanisms of dynamic cell membrane remodelling. *Nature* **438**, 590-596.

Mehlmann, L. M., Terasaki, M., Jaffe, L. A. and Kline, D. (1995). Reorganization of the endoplasmic reticulum during meiotic maturation of the mouse oocyte. *Dev. Biol.* **170**, 607-615.

Meyer, H. A., Grau, H., Kraft, R., Kosta, S. W., Prehn, S., Kalies, K. U. and Hartmann, E. (2000). Mammlian Sec61 is associated with Sec62 and Sec63. *J. Biol. Chem.* **12**, 14550-14557.

Munro, H. N. and Fleck, A. (1966). Recent developments in the measurement of nucleic acids in biological materials. A supplementary review. *Analyst* **91**, 78-88.

Nikonov, A. V., Snapp, E., Lippincott-Schwartz, J. and Kreibich, G. (2002). Active translocon complexes labeled with GFP-Dad1 diffuse slowly as large polysome arrays in the endoplasmic reticulum. *J. Cell Biol.* **158**, 497-506.

Orrenius, S. and Ericsson, J. L. (1966). Enzyme-membrane relationship in phenobarbital induction of synthesis of drug-metabolizing enzyme system and proliferation of endoplasmic reticulum. *J. Cell Biol.* **28**, 181-198.

Paiement, J., Dominguez, J. M., McLeese, J., Bernier, J., Roy, L. and Bergeron, M. (1990). Morphogenesis of endoplasmic reticulum in Xenopus oocytes after microinjection of rat liver smooth microsomes. *Am. J. Anat.* **187**, 183-192.

Palade, G. E. (1956). The endoplasmic reticulum. *J. Biophys. Biochem. Cytol.* **2**, 85-97.

Pedrosa Ribeiro, C. M., McKay, R. R., Hosoki, E., Bird, G. S. and Putney, J. W., Jr (2000). Effects of elevated cytoplasmic calcium and protein kinase C on endoplasmic reticulum structure and function in HEK293 cells. *Cell Calcium* **27**, 175-185.

Pierini, L., Holowka, D. and Baird, B. (1996). Fc epsilon RI-mediated association of 6-micron beads with RBL-2H3 mast cells results in exclusion of signaling proteins from the forming phagosome and abrogation of normal downstream signaling. *J. Cell Biol.* **134**, 1427-1439.

Rolls, M. M., Hall, D. H., Victor, M., Stelzer, E. H. and Rapoport, T. A. (2002). Targeting of rough endoplasmic reticulum membrane proteins and ribosomes in invertebrate neurons. *Mol. Biol. Cell* **13**, 1778-1791.

Rosenwald, A. G., Machamer, C. E. and Pagano, R. E. (1992). Effects of a sphingolipid synthesis inhibitor on membrane transport through the secretory pathway. *Biochemistry* **31**, 3581-3590.

Sandig, G., Kärgel, E., Menzel, R., Vogeli, F., Zimmer, T. and Schunk, W.-H. (1999). Regulation of endoplasmic reticulum biogenesis in response to cytochrome P450 overproduction. *Drug Metab. Rev.* **31**, 393-410.

Schweizer, A., Fransen, J. A. M., Bachi, T., Ginsel, L. and Hauri, H.-P. (1988). Identification, by a monoclonal antibody, of a 53kD protein associated with a tubulo-vesicular compartment at the cis-side of the Golgi apparatus. *J. Cell Biol.* **107**, 1643-1653.

Schweizer, A., Rohrer, J., Slot, J. W., Geuze, H. J. and Kornfeld, S. (1995). Reassessment of the subcellular localization of p63. *J. Cell Sci.* **108**, 2477-2485.

Snapp, E. L., Hegde, R. S., Francolini, M., Lombardo, F., Colombo, S., Pedrazzini, E., Borgese, N. and Lippincott-Schwartz, J. (2003). Formation of stacked ER cisternae by low affinity protein interactions. *J. Cell Biol.* **163**, 257-269.

Snapp, E. L., Reinhart, G. A., Bogert, B. A., Lippincott-Schwartz, J. and Hegde, R. S. (2004). The organization of engaged and quiescent translocons in the endoplasmic reticulum of mammalian cells. *J. Cell Biol.* **164**, 997-1007.

Subramanian, K. and Meyer, T. (1997). Calcium-induced restructuring of nuclear envelope and endoplasmatic reticulum calcium stores. *Cell* **89**, 963-971.

Takei, K., Mignery, G. A., Mugnaini, E., Sudhof, T. C. and De Camilli, P. (1994). Inositol 1,4,5-trisphosphate receptor causes formation of ER cisternal stacks in transfected fibroblasts and in cerebellar Purkinje cells. *Neuron* **12**, 327-342.

Terasaki, M. and Jaffe, L. A. (1991). Organization of the sea urchin egg endoplasmic reticulum and its reorganization at fertilization. *J. Cell Biol.* **114**, 929-940.

Terasaki, M., Song, J., Wong, J. R., Weiss, M. J. and Chen, L. B. (1984). Localization of endoplasmic reticulum in living and glutaraldehyde-fixed cells with fluorescent dyes. *Cell* **38**, 101-108.

Terasaki, M., Chen, L. B. and Fujiwara, K. (1986). Microtubules and the endoplasmic reticulum are highly interdependent structures. *J. Cell Biol.* **103**, 1557-1568.

Terasaki, M., Slater, N. T., Fein, A., Schmidek, A. and Reese, T. S. (1994). Continuous network of endoplasmic reticulum in cerebellar Purkinje neurons. *Proc. Natl. Acad. Sci. USA* **91**, 7510-7514.

Terasaki, M., Runft, L. L. and Hand, A. R. (2001). Changes in organization of the endoplasmic reticulum during Xenopus oocyte maturation and activation. *Mol. Biol. Cell* **12**, 1103-1116.

Thomas, J. L., Holowka, D., Baird, B. and Webb, W. W. (1994). Large-scale co-aggregation of fluorescent lipid probes with cell surface proteins. *J. Cell Biol.* **125**, 795-802.

Voeltz, G. K., Rolls, M. M. and Rapoport, T. A. (2002). Structural organization of the endoplasmic reticulum. *EMBO Rep.* **3**, 944-950.

Voeltz, G. K., Prinz, W. A., Shibata, Y., Rist, J. M. and Rapoport, T. A. (2006). A class of membrane proteins shaping the tubular endoplasmic reticulum. *Cell* **124**, 573-586.

Vogel, F., Hartmann, E., Gorlich, D. and Rapoport, T. A. (1990). Segregation of the signal sequence receptor protein in the rough endoplasmic reticulum membrane. *Eur. J. Cell Biol.* **53**, 197-202.

Vunnam, R. R. and Radin, N. S. (1980). Analogs of ceramide that inhibit glucocerebroside synthetase in mouse brain. *Chem. Phys. Lipids* **26**, 265-278.

Waterman-Storer, C. M. and Salmon, E. D. (1998). Endoplasmic reticulum membrane tubules are distributed by microtubules in living cells using three distinct mechanisms. *Curr. Biol.* **8**, 798-806.

Weibel, E. R., Staubli, W., Gnagi, H. R. and Hess, F. A. (1969). Correlated morphometric and biochemical studies on the liver cell. I. Morphometric model, stereologic methods, and normal morphometric data for rat liver. *J. Cell Biol.* **42**, 68-91.